第 19 卷第 2 期
2000 年 4 月

红外与毫米波学报
J. Infrared Millim. Waves

Vol. 19, No. 2
April, 2000

COMPARISON OF CHARACTERIZATION TECHNIQUES IN P-ON-N HgCdTe LWIR PHOTODIODES TECHNOLOGY *

WENUS Jakub MADEJCZYK Pawel RUTKOWSKI Jaroslaw
(Institute of Applied Physics, Military University of Technology, 2 Kaliskiego Str., 00-908 Warsaw, Poland)

Abstract In this paper standard techniques for characterization of HgCdTe liquid phase epitaxial layers (LPE) were presented. The performance of long wavelength p-on-n HgCdTe photodiodes fabricated by arsenic diffusion was described. The correlation between LPE HgCdTe material parameters and properties of the infrared photodiodes was demonstrated.

Key words HgCdTe LPE growth, methods of material characterization, p-on-n HgCdTe LWIR photodiodes.

Introduction

At present HgCdTe is the most widely used variable-gap semiconductor for infrared (IR) photodetectors. Over the years it has successfully fought off major challenges from extrinsic silicon and lead-tin telluride devices despite that it has more competitors today than ever before. These include Schottky barriers on silicon, SiGe heterojunctions, AlGaAs multiple quantum wells, GaInSb strained layer superlattices, high temperature superconductors and especially two types of thermal detectors: pyroelectric detectors and silicon bolometers. It is interesting, however, that none of these competitors can compete in terms of fundamental properties.[1,2] They may promise to be more manufacturable, but never to provide higher performance or, with the exception of thermal detectors, to operate at higher or even comparable temperatures.

Recently, more interest has been focused on HgCdTe photodiodes. Photodiodes with very low power dissipation and easy multiplexing on focal plane silicon chip, can be assembled in two-dimensional arrays containing a very large ($\approx 10^6$) number of elements, limited only by existing technologies. Liquid phase epitaxy is one of the basic methods for growing device quality HgCdTe material.

In this paper standard techniques for characterization of $Hg_{1-x}Cd_xTe$ ($0.20 < x < 0.25$) liquid phase epitaxial (LPE) layers are presented. Backside-illuminated p-on-n photodiodes have been fabricated by arsenic diffusion. The correlation between LPE HgCdTe material parameters and properties of the infrared photodiodes is demonstrated. We have chosen to limit the scope of this paper to electrical and optical characterization techniques. We emphasize those characterization techniques that are proved to be the most helpful and useful in device processing.

1 Characterization of LPE Layers

The LPE layers as a starting material for device fabrication have been characterized by several techniques. Selection of material for devices requires a method that can determine composition uniformity of epitaxial layers. IR transmission measurements are possibly the most common routine method to determine the composition x of $Hg_{1-x}Cd_xTe$ wafers. The main reason of extensive use of IR transmission measurements is the fact that it is a non-destructive method. The IR transmission measurements were

* The project supported by the KBN(Poland) under contract No PBZ 28.11/P6
Received 1999-09-09, revised 1999-10-20

* 波兰 KBN(PBZ 28.11/P6)资助项目
稿件收到日期 1999－09－09，修改稿收到日期 1999－10－20

performed on a SPECTRUM 2000 FTIR Spectrometer at room temperature. The FTIR measurement has numerous advantages: it has mapping capability, it is contactless and non-destructive, and it accurately predicts cut-off wavelengths, determines layer thickness, and is thus capable of determining the x-value and composition profiles of epitaxial layers.[3]

The electrical properties of the starting HgCdTe wafers were routinely determined by Hall effect in the temperature range between 77K and 300K. The measurements were carried out on Van der Pauw samples fabricated from representative wafers selected from all wafers. Discussion of the Hall effect measurements has become an excellent process monitor for LPE growth with the purity, doping and homogeneity able to be correlated with growth conditions.

Determination of dopant concentration in solid involves the use of Hall effect measurements as well as corroboration with second ion mass spectrometry (SIMS) concentration profiles. The correspondence in the concentration of a dopant measured by SIMS and Hall effect or capacitance-voltage (C-V) methods is indication of activity of that dopant. Measurements on the same sample by the two techniques were used to unequivocally substantiate the electrical activity of impurity dopants.

Temperature dependence of the excess carrier lifetime of HgCdTe wafers has been measured by the photoconductive decay method on the Van der Pauw Hall sample.

2 Device Fabrication and Characterization

The backside-illuminated p-on-n HgCdTe homojunction photodiodes were fabricated using LPE layers grown on an IR-transparent CdZnTe substrate. The LPE system and procedures employed here have been previously reported[4]. The carrier concentration in 10—15μm thick n-type was controlled in the range (2—4)$\times 10^{15}$cm^{-3} using indium doping. The p^+-n junctions were formed by arsenic diffusion. The As dopants must reside on the Te site to accomplish p-doping. This requires either growth or annealing at relatively high temperature under cation-rich conditions. The annealing procedure was carried out at 430℃ for 2h by placing the wafer in a closed quartz ampoule with Hg and As sources. After the diffusion, the crystals were additionally annealed in saturated mercury vapor pressure at 260℃ for further reduction of native point defects by annihilation of Hg vacancies that were previously encountered, revealing the net doping due to impurity n-type background. Typically, the p-n junctions were located at a depth of 1μm (from the surface), and the carrier concentrations in p-type surface layers were about 5×10^{17}cm^{-3}. Then, the photodiodes were delineated by a mesa etch through the thin cap layer, passivated, and finally metal contacts were formed.

The photodiode performance was established by measurements of the current-voltage (I-V) characteristics, capacity-voltage (C-V) characteristics, and spectral responsivity at 77K. The photodiodes were mounted in a liquid nitrogen cooled cryostat system and the temperature dependence of characteristics was measured in the temperature range between 77K and 300K. The relative photoresponse spectra were measured with a FTIR spectrometer. The absolute photoresponse was determined using a calibrated blackbody test set, which is composed of a blackbody source, preamplifier, lock-in amplifer, and chopper system. Capacitance and conductance of photodiode were measured as a function of bias voltage using Keithley 590C impedance analyzer.

3 Correlation between Alloy Composition and Cut-off Wavelength of the Photodiode

Determination of the wafer composition (x value) is crucial for controlling and monitoring growth processes. It has become common to determine the $Hg_{1-x}Cd_xTe$ composition x and to predict detector cut-off wavelength from the cut-on wavelength measured at 300K by IR transmission, usually at several points on a wafer. Different manufacturers generally use different features of the IR transmission spectra. The cut-off wavelength is usually defined as the wavelength where the response of the detector falls to 50% of the peak value. The approximation is usually made that the cut-off wavelength

Table 1 Composition of epilayer No. S2 using different methods of IR transmission spectra measurements.

Sample S2	Corner 1	Corner 2	Corner 3	Corner 4	Centre
Composition x calculated from $Z_{1/2}$	0.2032	0.2044	0.2036	0.2035	0.2021
Composition x calculated from Z_{500}	0.2039	0.2055	0.2045	0.2046	0.2030
Composition x calculated from Z_{1000}	0.2036	0.2060	0.2043	0.2042	0.2019
Accuracy of measurement Δx	0.0017	0.0012	0.0024	0.0019	0.0022

(λ_c) occurs at E_g ($\lambda_c = 1.24/E_g$) and many publications have reported equations which determine E_g from x value and temperature. The cut-on wavelength has been determined by a variety of methods from the specific wavenumbers: $Z_{1/2}$ of the 50% maximum transmission, Z_{500} of the 500cm^{-1} absorption coefficient and Z_{1000} of the 1000cm^{-1} absorption coefficient. The composition of an epilayer can be calculated using the above wavenumbers. To determine the wavenumbers Z_{500} and Z_{1000}, the relationship between epilayer thickness and transmission values can be obtained from Ref. [5]. To check the accuracy of x determination by FTIR measurement, composition was calculated from the above three described methods. Results gathered in Table 1 show that these comparisons indicated excellent absolute x agreement between 50% transmission, 500cm^{-1} and 1000cm^{-1} absorption measurements. The accuracy of the calculated compositions using three wavenumbers obtained from the measured IR transmission curve is less than 0.002, which is in the range of instrumental measurement error. An example of typical FTIR data is shown in Fig. 1.

Measurements performed by FTIR spectrometers give both composition and thickness mapping capability over the layer area. It appears that composition x is more homogeneous than thickness d of the layer. Table 1 summarizes the measurement accuracy for five points of the sample. Two criteria were used for evaluation of accuracy. The first is the relative accuracy, which indicates the resolution of measuring changes in composition. The highest accuracy is obtained when consecutive measurements are performed on the same sample. Higher accuracy requires longer measurement time (more number of scans, longer optical path difference). The second criterion is the accuracy of thickness determination. The thickness of the sample was determined from the interference peaks. The method presented here includes the change of refractive index with wavelength and averages of the data using least-squares $m = 2dn\nu$, where m is the integer number of interference peaks, n is the refractive index of HgCdTe, and ν is the wavenumber. The resolution of thickness measurements is a function of the diameter of the incident light spot on the sample. Small spot diameter has been obtained with successful results but the signal-to-noise ratio was reduced. The interference peaks as

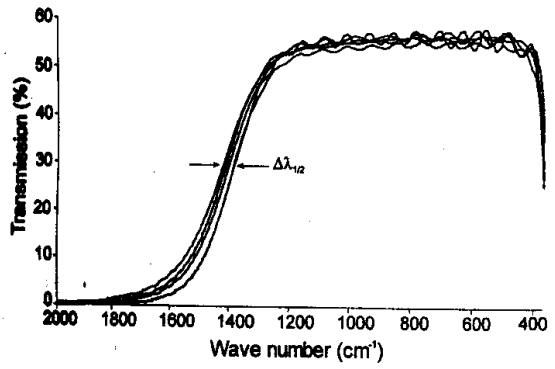

Fig. 1 Typical transmission spectra for $Hg_{0.8}Cd_{0.2}Te$ LPE layer at several points over the wafer area

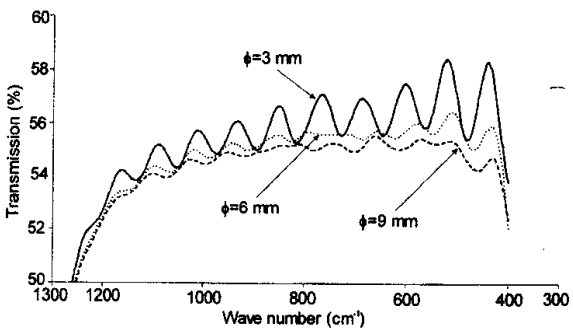

Fig. 2 Transmission spectra for $Hg_{0.8}Cd_{0.2}Te$ LPE layer as a function of the light spot diameter

a function of the diameter of the light spot are illustrated in Fig. 2.

The cut-off wavelength of HgCdTe photodiode is determined not only by energy gap. In addition, it is dependent upon the thickness of the layer, the diffusion length of the minority carriers, compositional profile of the layers, mesa depth, size of the diode and backside reflection coefficient. Due to the large number of factors affecting λ_c, empirical equations determined from cut-on wavelength measurements at 300K and λ_c measurements at the temperature of interest, can be used to determine accurately the predicted cut-off wavelength. However, there is no one equation, which applies to all photodiodes. The following equation was determined from the data taken from FTIR cut-on wavelength measurements using 50% transmission method and cut-off photodiode wavelengths measured at 77K:

$$\lambda_c(77\mathrm{K}) = 1.54 \times \lambda_{50\%}(300\mathrm{K})$$

This equation is valid only for p-on-n device structures with base layer thickness of 15μm, and standard diffusion parameters (time 4h, temperature 700K). Even so, the results still vary with changes in diode geometry, passivation and other diffusion parameters. The example of FTIR transmission and spectral characteristic of diodes is shown in Fig. 3. The transmission curve measured after As diffusion is shifted towards shorter wavelengths due to reasonably high temperature (430℃) of the diffusion process, which causes changes in x value. The determing of predicted cut-off wavelengths and measured λ_c are shown in Table 2.

Table 2 Comparison of HgCdTe photodiode cut-off wavelengths obtained by different methods

Sample Tel2	λ_c(μm)
From transmission curve before As diffusion	12.3
From transmission curve after As diffusion	10.6
From photodiode spectral characteristic	10.3
From R_0A vs temperature	11.9

Optical reflectance measurements are useful for characterizing the surface x value of material. Analysis of the alloy composition determined from reflection UV measurements shows that the lateral homogeneity of the as-grown LPE layers is very good. After As diffusion the UV reflection measurements have not been done because the changes of post-annealing HgCdTe surface affect the peak reflectivity location. The carrier concentration may also give rise to apparent composition change due to Moss-Burstein shift. For several layers, the composition profiles in the direction perpendicular to the surfaces were obtained by step-removing surface layers. The obtained results show that the depth homogeneity is also very good, except for a narrow region of graded composition adjacent to the substrate. The functional dependence of peak reflectivity location on x for HgCdTe has been taken from Ref. [6]. Relative resolution of composition measurements is 0.005. This accuracy is limited by the broad peaks and the surface treatment in step-removing. The composition determined by IR transmission measurements was compared with an

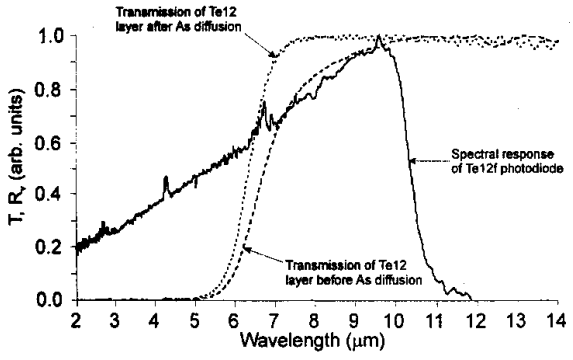

Fig. 3 Comparison of FTIR transmission and spectral responsivity of $Hg_{0.79}Cd_{0.21}Te$ photodiode

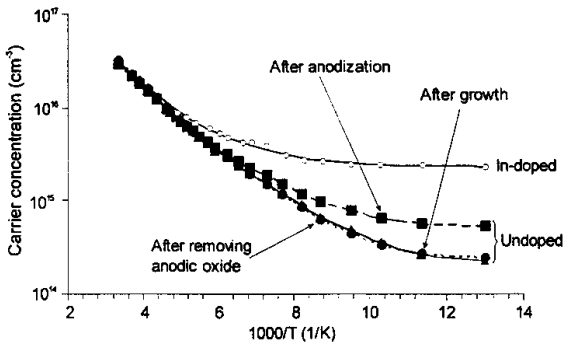

Fig. 4 Effects of surface treatment on temperature dependence of the carrier concentration for doped and undoped $Hg_{0.8}Cd_{0.2}Te$

average of 5 reflectance measurements mapped across the wafers. This gave $x=0.215$ and $x=0.220$ for IR transmission and reflectance, respectively.

IR transmission measurements are used more widely than optical reflectance for predicting device cut-off wavelength and determining layer thickness. FTIR measurements, however, have some disadvantages: small spatial or depth resolution and measurements usually dominated by the smallest bandgap region in the sample.

4 Carrier Concentration and Doping Profile of the Photodiode

Hall effect and conductivity measurements indicate, in general, that longer wavelength material and high-purity samples show a frequent occurrence of anomalous results. The classical results are mostly found for shorter wavelength material and in intentionally doped samples. Representative classical Hall-effect curves are shown in Fig. 4. In the n-type material two distinct regions are observed; namely, the intrinsic region and the extrinsic exhaustion region. In the extrinsic region, the Hall coefficient R_H is a constant; then the donor levels can be estimated using the formula $n=-1/R_Hq$.

In addition to bulk electron densities and mobilities, one can determine inversion or accumulation layer properties. The behavior of Hall curves strongly depends on surface treatment of the sample. A freshly etched sample showed classical n-type Hall coefficient and mobility. After anodization the same sample showed higher electron concentration as a result of a thin skin n-type material induced on surface of the sample. In-doped samples, used in device technology, have electron concentration about $3\times10^{15}\text{cm}^{-3}$ and mobility $4\times10^{4}\text{cm}^2/\text{Vs}$.

In addition, capacitance-voltage (C-V) measurements on large diode structures were performed in order to compare with the Hall effect measurements (see Fig. 5). For a p-on-n structure, the calculated carrier concentration distribution is mostly on the n-type side. The depletion width at zero bias is typically 0.2μm and the junction appears to be abrupt. The doping concentration at zero bias is about 2×10^{15} cm^{-3} and usually is lower than obtained from Hall effect data. This is probably result of compensation, which takes place at the p-n junction interface.

The differential Hall measurements show that thin p^+ layer has hole concentration about 1×10^{17} cm^{-3} and the based 10μm thick layer with electron concentration $2\times10^{15}\,\text{cm}^{-3}$. This differential Hall technique is not good enough to the accuracy of carrier concentration determination, because its resolution is rather poor (20%). The doping profiles of the photodiodes were obtained by SIMS technique. An example of 15μm thick LPE-grown HgCdTe structure after As diffusion is shown in Fig. 6. The arsenic profile shows significant diffusion of 1.5μm and an approximate Gaussian profile. The relative alloy composition in this layer was measured by the Te

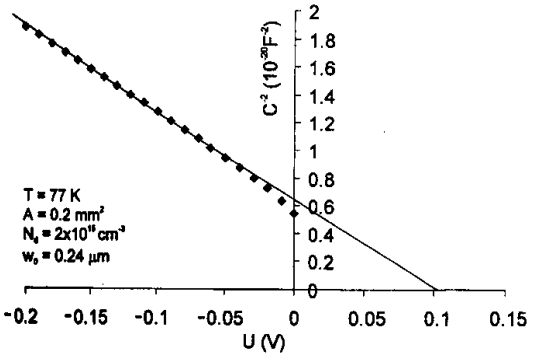

Fig. 5 1 MHz C-V characteristic of p^+-n HgCdTe photodiode at 77 K

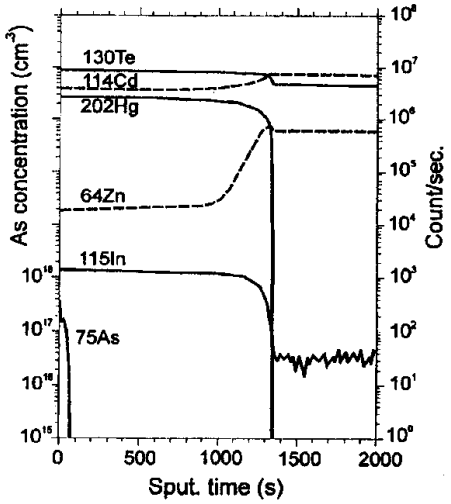

Fig. 6 The SIMS profile of As in a $Hg_{0.79}Cd_{0.21}Te$ epitaxial layer after low-temperature annealing

secondary ion yield. Figure 6 shows that, even at the relatively high doping level of 2×10^{17}atoms/cm^3, no significant change in the composition is observed. SIMS analysis of In doping level and 77K Hall effect measurements of the n-type carrier concentration show full activation of In. To determine the p-type doping concentration and activation energy of arsenic in layers, variable temperature Hall measurements have been performed to determine the arsenic activation energy and the degree of compensation.

5 Photodiode Performance and Carrier Lifetime of Samples

Figure 7 shows the forward bias I-V curves of p-on-n diodes at 77K in low background flux condition. For bias voltage $V>10$mV, the I-V characteristic is exponential with a slope $(qV/\beta kT)$, where the ideality factor $\beta=1.2$ for better photodiodes ($x=0.21$). When tunneling current dominates, the ideality factor increases beyond 2($x=0.25$). For $V>70$mV the forward characteristic is a double exponential with $\beta=1.9$, which indicates that the g-r current dominates. Thus an analysis of the forward bias current-voltage curves gives very important information of dominating current mechanism and allows estimating the quality of starting material.

The most widely used figure of merit to characterize both the dark current and the thermal noise of an infrared photodiode is the R_0A product. It is defined as the product of the diode resistance R_0 at zero bias voltage and the photodiode active area A. Figure 8 shows the dynamic resistance-area product as a function of bias voltage at 77K. The dark as well as the background-illuminated characteristics are shown.

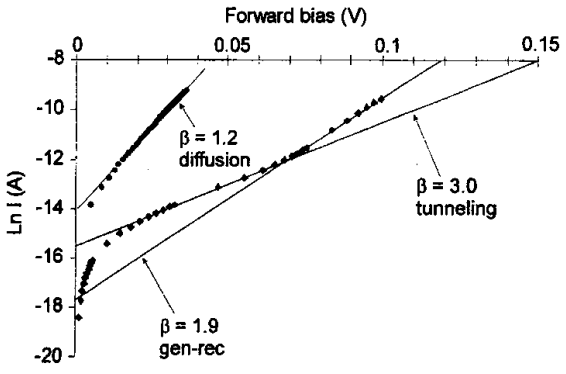

Fig. 7 Forward bias I-V characteristics of $Hg_{1-x}Cd_xTe$ photodiodes at 77 K, ● $x=0.21$, ♦ $x=0.25$

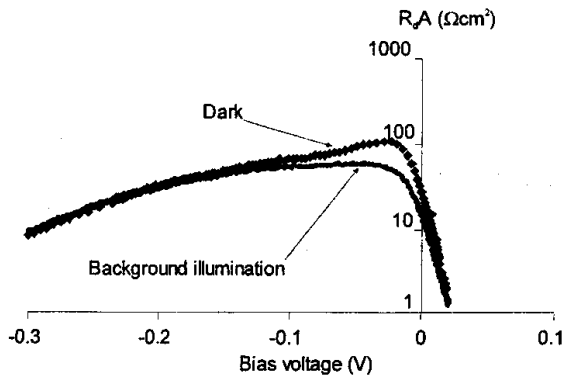

Fig. 8 R_dA product as a function of bias voltage for $Hg_{0.79}Cd_{0.21}Te$ photodiode at 77 K under zero field of view and at 300 K background

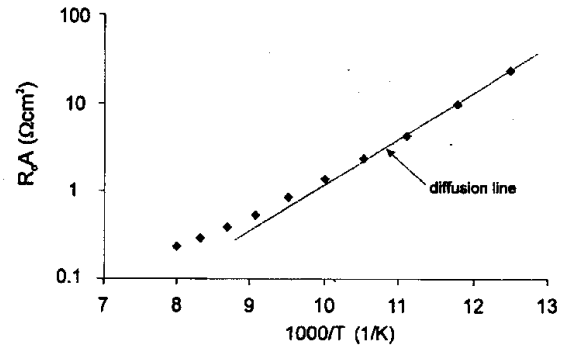

Fig. 9 R_0A product as a function of temperature for $Hg_{0.79}Cd_{0.21}Te$ photodiode

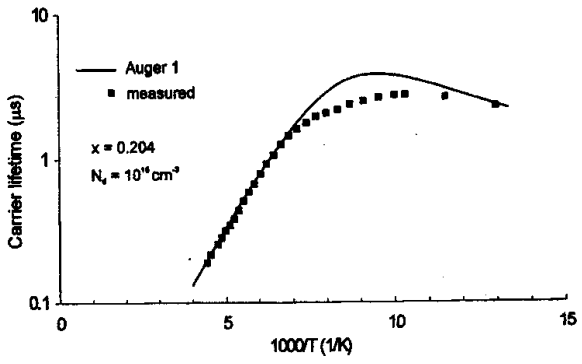

Fig. 10 Measured minority carrier lifetime versus reciprocal temperature for LPE grown HgCdTe layer

Decrease of the R_0A product with the increase of background illumination is typical for these photodiodes. The R_0A product as a function of temperature is shown in Fig. 9. The devices were diffusion-current limited down to 77K. A theoretical one-dimensional R_0A model was used to calculate diffusion current of n-side active layer[7]. The measured material parameters such as the x value, thickness of active layer and carrier concentration were utilized as input parameters to the model. The band gap value of E_g = 100 meV was deduced from the temperature dependence of the R_0A product. The cut-off wavelength calculated from this dependence is longer than the one obtained from optical measurements as shown in Table 2. Discrepancies are caused mainly by inaccuracy in temperature and R_0A product measuring. The cut-off wavelength obtained from transmission curve after As diffusion is in good agreement with this value measured from photodiode spectral characteristic.

The minority carrier lifetime is an important parameter for the materials. Temperature dependence of the excess lifetime for HgCdTe sample before As diffusion is shown in Fig. 10. The experimental data (solid symbol) agree well with a theoretical model (solid line), that includes Auger-1 recombination mechanisms. The minority carrier lifetime for Auger recombination process calculated from R_0A product at 77K is equal to 2μs, so agreement between sample parameters and detector performance is excellent. The above results suggest that the starting material parameters are not degraded during the technological steps of photodiode fabrication.

6 Conclusion

In the paper standard techniques for characterization of LPE HgCdTe layers are presented. The starting material for photodiode fabrication has been characterized using different methods of measurements: FTIR measurements, the Hall effect measurements, C-V analysis, SIMS analysis and excess carrier lifetime measurements. Backside-illuminated p-on-n photodiodes have been fabricated by arsenic diffusion. The performance of $Hg_{0.79}Cd_{0.21}Te$ photodiodes is diffusion limited down to 77K. The R_0A product higher than 10Ωcm^2 at liquid nitrogen temperature has been obtained. Particular attention has been put on the correlation between LPE HgCdTe material parameters and properties of the infrared photodiodes. Three types of measurements have been reviewed in more detail. Correlation between alloy composition and cut-off wavelength of the photodiode, carrier concentration and doping profile of the photodiode, carrier lifetime and R_0A product of photodiode have been shown. Results of the paper indicate that the starting material parameters are not degraded during the technological steps of photodiode fabrication.

REFERENCES

[1] Adamiec K, Rogalski A, Rutkowski J. Progress in infrared detector technology, *J. Tech. Phys.*, 1997, **38**: 431—488

[2] Piotrowski J, Rogalski A. New generation of infrared photodetectors, *Sensors and Actuators.*, 1998, A**67**: 146—152

[3] Seiler D G, Mayo S, Lowney J R. $Hg_{1-x}Cd_xTe$ characterization measurements: current practice and future needs, *Semicond. Sci. Technol.*, 1993, **8**: 753—776

[4] Adamiec K, Rutkowski J, Rogalski A, *et al.* Comparison of mercury cadmium telluride LPE layers growth from Te-rich solution on (111) $Cd_{0.95}Zn_{0.05}Te$ and (211) $Cd_{0.95}Zn_{0.05}Te$, *Proc. SPIE.*, 1999, **3629**: 88—97

[5] Jeoung Y, Lee T, Kim H, *et al.* New method of the determination of HgCdTe/CdZnTe composition by infrared transmission, *J. Appl. Phys.*, 1996, **35**: 134—139

[6] Price S L, Boyd P R. Overview of compositional measurement techniques for HgCdTe with emphasis on IR transmission, energy dispersive x-ray analysis and optical reflectance, *Semicond. Sci. Technol.*, 1993, **8**: 842—859

[7] Rogalski A. Analysis of the R_0A product in n^+-p $Hg_{1-x}Cd_xTe$ photodiodes, *Infrared Phys.*, 1988, **28**: 139—153

WENUS Jakub *et al.*: Comparison of characterization techniques in p-on-n HgCdTe LWIR photodiodes technology
WENUS Jakub *et al.*: Comparison of characterization techniques in p-on-n HgCdTe LWIR photodiodes technology